Carbohydrate Polymers 87 (2012) 101–109

Contents lists available at ScienceDirect

Carbohydrate Polymers

journal homepage: www.elsevier.com/locate/carbpol

Biodegradable and biocompatible polyampholyte microgels derived from chitosan, carboxymethyl cellulose and modified methyl cellulose

Neha Dhar, Seyedeh Parinaz Akhlaghi, Kam C. Tam*

Department of Chemical Engineering, Waterloo Institute for Nanotechnology, University of Waterloo, 200 University Avenue West, Waterloo, Ontario, Canada N2L 3G1

ARTICLE INFO

Article history:
Received 31 March 2011
Received in revised form 6 June 2011
Accepted 13 July 2011
Available online 29 July 2011

Keywords:
Polyampholyte microgels
Chitosan
Carboxymethyl cellulose (CMC)
Methyl cellulose
pH-responsive
Thermo-responsive

ABSTRACT

Two biocompatible and biodegradable polyampholyte microgels, namely chitosan–carboxymethyl cellulose (CS–CMC) and chitosan–modified methyl cellulose (CS–ModMC) were synthesized by an inverse microemulsion technique. The CS–CMC microgel system was pH-responsive while the CS–ModMC system possessed both pH and thermo-responsive properties. For CS–CMC system, the number of $-OCH_2COOH$ and $-NH_2$ groups was determined to be 1.5 and 1.1 meq/g of microgel, respectively. In the pH range of 4–9, the zeta potential values varied from +10 to −40 mV, while the hydrodynamic radius varied from 160 nm in the swollen state (acidic and basic pH) to 110 nm in the "collapse" state (neutral pH). Furthermore, TEM micrographs confirmed the swelling/deswelling behaviour of CS–CMC microgel particles at acidic, neutral and basic conditions. For CS–ModMC system, the number of $-OCH_2COOH$ and $-NH_2$ groups was determined to be 0.8 and 0.6 meq/g microgel, respectively. In the pH range of 4–9, the surface charge on the microgels varied from +25 to −60 mV and the hydrodynamic radii were 190 nm at low pH, 80 nm at neutral pH, to 120 nm at a high pH. In vitro drug release studies confirmed that CS–CMC microgels could encapsulate and release a model drug, thus they could potentially be used as biocompatible and biodegradable drug carriers.

1. Introduction

Polyampholytes are defined as polymers capable of possessing both positive and negative charges on their backbones. The properties of polyampholytes are dependent on intra-chain electrostatic interactions since both negative and positive charges are present on the same backbone (Neyret & Vincent, 1997). Polyampholytes differ from polyelectrolytes in the sense that polyelectrolytes may possess *either* positive *or* negative charges on their backbones, however polyampholytes possess *both* charges on the same backbone. Microgels on the other hand are crosslinked polymer particles with sizes ranging from 100 nm to 1 μm, and they swell in a good solvent (Das & Kumacheva, 2006). Microgels possess functional properties, and depending on the constituent polymers, they exhibit different stimuli-responsive behaviour (swelling/deswelling behaviour) in response to pH, temperature, ionic strength, solvent and external magnetic field (Tan & Tam, 2008). By combining the properties of '*polyampholyte*' and '*microgel*' we obtain a new class of microgel called '*polyampholyte microgel*'. This microgel possesses positive and negative charges, arising from the pH dependent amines and carboxylic acids. At low pH, the amino groups become protonated and acquire positive charges while at high pH, carboxylic acid groups become deprotonated and acquire negative charges.

The primary reason for synthesizing polyampholyte microgels is that their pH responsive behaviour will be attractive for drug and protein delivery applications. Ho, Tan, Tan, and Tam (2008) synthesized polyampholyte microgels using poly(methacrylic acid) (PMAA) and poly(2-(dimethylamino)ethyl methacrylate) (PDMA). Inverse microemulsion polymerization technique was used to polymerize MAA and DMA in the presence of a cross-linker (allyl methacrylate) to produce an amphoteric microgel system. The microgels exhibited swelling at low and high pH while they deswelled at neutral pH. At low and high pH, the microgel particles acquire positive and negative charges, respectively and the particles begin to swell due to the osmotic pressure from counter ions and repulsion from like charges within the microgel particles. Conversely, as the solution approaches a neutral pH, equal number of positive and negative charges on the microgel particles results in a smaller hydrodynamic radius as the counterions leave the microgel particles causing them to deswell. Due to the overall charge neutralization on the surface of the microgel, the particles tend to flocculate at the isoelectric point (IEP). In order to prevent flocculation at IEP, a steric stabilizer, such as poly (ethylene glycol) methacrylate (PEGMA) was grafted on the microgels (Ho et al., 2008; Tan, Ravi, Tan, & Tam, 2007).

* Corresponding author.
E-mail address: mkctam@uwaterloo.ca (K.C. Tam).

0144-8617/$ – see front matter © 2011 Elsevier Ltd. All rights reserved.
doi:10.1016/j.carbpol.2011.07.022

Recently, many different polyampholyte microgel systems have been examined (Christodoulakis & Vamvakaki, 2010; Schachschal et al., 2010; Wang, Zhang, Wang, Sun, & Shen, 2010; Xu et al., 2010). Due to their potential applications and stimuli responsive characteristics, we have synthesized polyampholyte microgels from biopolymers instead of synthetic polymers. In our approach, we utilize water-soluble polymers dispersed in a continuous organic phase together with a water-soluble crosslinker, such as 1-ethyl-3-(3-dimethylaminopropyl) carbodiimide (EDC), to produce crosslinked microgels. This synthetic technique is akin to inverse microemulsion polymerization (IMEP). Simple EDC carbodiimide chemistry was used to crosslink amino and carboxylic acid groups through amide linkages (Nakajima & Ikada, 1995). Inverse microemulsions are thermodynamically stable water-in-oil (W/O) emulsions formed by adding large amounts of surfactants (Oh, Drumright, Siegwart, & Matyjaszewski, 2008). Inverse microemulsion technique is especially useful for water-soluble polymers that tend to polymerize in the aqueous phase. Water droplets in a W/O inverse microemulsion act as nanoreactors, thereby allowing encapsulation and crosslinking of water-soluble polymeric chains in the water nano-droplets.

Non-ionic surfactants are required to produce inverse microemulsions because of their unique phase-inversion characteristic. Non-ionic surfactants transform an oil-in-water (O/W) emulsion at room temperature to water-in-oil (W/O) emulsion at higher temperatures. The temperature, at which phase-inversion occurs for the transformation of an O/W to W/O emulsion is called the phase inversion temperature (PIT). The PIT is a strong function of the hydrophile–lipophile balance (HLB) of surfactants, which corresponds to the ratio of hydrophilic (water-loving) to lipophilic (oil-loving) segments on a surfactant. Mixing two non-ionic surfactants with different HLB values produces a desired HLB value to yield the desired PIT (Lehnert, Tarabishi, & Leuenberger, 1994). Thus, by mixing appropriate amounts of two non-ionic surfactants, a HLB value that gives rise to a desired phase inversion temperature can be achieved.

We have synthesized polyampholyte microgels composed of biodegradable polymers, namely chitosan, carboxymethyl cellulose and methyl cellulose that are derived from natural sources, such as chitin and cellulose. Chitosan (CS) is obtained by the deacetylation of chitin (Rinaudo, 2008), carboxymethyl cellulose (CMC) from carboxymethylation of cellulose (Heinze & Koschella, 2005) and methyl cellulose (MC) from methylation of alkali cellulose (Mansour, Nagaty, & Elzawawy, 1994). Two different polyampholytic systems were explored: chitosan–carboxymethyl cellulose (CS–CMC) and chitosan–modified methyl cellulose (CS–ModMC). In the first system, chitosan and carboxymethyl cellulose were chosen since they would impart amino and carboxylic acid functionalities to the microgels. As a further extension of the CS–CMC system, we have also synthesized chitosan–modified methyl cellulose system where the methyl cellulose was modified by carboxymethylation (Heinze & Koschella, 2005) to incorporate carboxylic acid functionality to the microgels. Methyl cellulose contains methoxide groups, and the hydrophobic interaction between methoxide groups induces chain association at the lower critical solution temperature (LCST) (Chevillard & Axelos, 1997). Thus, by combining the pH responsive characteristics of chitosan and thermo-responsive behaviour of methyl cellulose, a bi-responsive system was produced. The advantages of using these naturally derived polyampholyte microgels are:

- The microgels are biodegradable and biocompatible (Chen & Fan, 2008; Rinaudo, 2008; Yoon et al., 2006)
- They are non toxic and non allergenic (Samir, Alloin, & Dufresne, 2005)
- They are readily available and cheap as they are derived from renewable resources, which can be recycled (Samir, Alloin, & Dufresne, 2005)
- Using polymers as starting material instead of synthetic monomers ensure that toxic initiators are absent in the products, making them suitable for biomedical and pharmacological applications (Agnihotri, Mallikarjuna, & Aminabhavi, 2004; Kamel, Ali, Jahangir, Shah, & El-Gendy, 2008)

2. Materials and methods

2.1. Materials

Chitosan (M.W. 50,000–190,000, D.S ~75–80%) was purchased from Aldrich. Sodium salt of carboxymethyl cellulose (CMC-Na M.W. 250,000, D.S-1.2) was purchased from Acros Organics. Methyl cellulose (water-soluble gum) was purchased from Fisher Scientific. Monochloroacetic acid (solid flakes, 99%) was purchased from Acros and used for the carboxymethylation of methyl cellulose. EDC (1-ethyl-3-(3-dimethylaminopropyl) carbodiimide, commercial grade) and NHS (*N*-hydroxysuccinimide, 98%+) were purchased from Sigma and Acros Organics, respectively. MES (2-(*N*-morpholino) ethanesulfonic acid, >99%) was used as buffer for the EDC crosslinking reaction and was purchased from Aldrich. Non-ionic surfactants Brij 92V and Brij 96V were purchased from Aldrich and Fluka, respectively and used as received. For steric stabilization, poly (ethylene glycol) methacrylate (PEGMA M.W. 300 Da, inhibitors removed using basic alumina) was purchased from Sigma and tert-butyl hydroperoxide initiator (TBHP, 70% solution in water, N_2 flushed) was purchased from Acros Organics. Millipore deionized water was used for all the experiments and sample preparations.

2.2. Synthesis of chitosan–carboxymethyl cellulose microgels

In the synthesis of CS–CMC microgels, a surfactant mixture was first prepared by mixing 30 mL of hexane with 0.552 g of Brij 96 (HLB ~ 12.4) and 1.848 g of Brij 92 (HLB ~ 4.9) surfactants. The combined HLB of this system was ~6.625 yielding a phase inversion temperature of around 70 °C (Ho et al., 2008). This surfactant mixture was added to a 100 mL (three necked) round bottom reaction vessel and the temperature was raised to 70 °C. 0.05 g chitosan was dissolved in 10 mL of 1% acetic acid solution and 0.03 g of CMC-Na (sodium salt of carboxymethyl cellulose) was dissolved in 10 mL of DI water. The pHs of both polymer solutions were adjusted to 5, since EDC crosslinker works more effectively in the pH range of 4–6 (Nakajima & Ikada, 1995). 0.1 wt% MES buffer was added to each polymer solution to maintain the pH at a constant value. Then, 0.016 g of EDC and 0.01 g of NHS was added to the chitosan solution. The EDC/NHS loaded chitosan solution and CMC-Na solution were added simultaneously to the surfactant mixture in the reaction vessel. As soon as the polymers were added, the solution turned turbid, and the reaction was allowed to proceed for another 4 h. Free radical grafting method was used to graft steric stabilizers on the surface of the microgels. 0.1 mL of 1% TBHP solution and 0.2 g of PEGMA-300 was added to the reaction vessel under N_2 purge. The grafting reaction was allowed to continue for another hour. In order to remove the hexane, the hot reaction mixture was poured into a rotary evaporator and hexane was removed under vacuum. The resulting microgel sample was diluted with DI water and dialyzed (M.W cut off: 10,000 Da) for about a week to remove surfactants, initiator, unreacted polymers and any homopolymers of PEGMA that may have formed during the grafting reaction.

2.3. Modification of methyl cellulose

In order to incorporate carboxylic acid groups on methyl cellulose chains, carboxymethylation was used for the chemical modification. Carboxymethylation of methyl cellulose was carried out using a standard slurry process (Heinze & Pfeiffer, 1999). 0.5 g of methyl cellulose powder was suspended in 15 mL of isopropanol through vigorous stirring. 1.33 mL of 15% (w/v) NaOH solution was added drop wise into the suspension. The stirring was continued for another hour before adding 0.6 g of monochloroacetic acid. The reaction mixture was heated to 55 °C for about 1.5 h, and the reaction time was controlled to prevent depolymerisation of methyl cellulose. The product was recovered from the suspension, using acetone as the non-solvent. The powder-like product was washed with acetone and 80% (v/v) ethanol solution several times and then dried under vacuum at 60 °C.

2.4. Synthesis of chitosan–modified methyl cellulose microgels

As described in Section 2.2, the same experimental procedure was used to synthesize the CS–ModMC microgels, incorporating modified methyl cellulose instead of carboxymethyl cellulose. It was also observed that the modified methyl cellulose powder dissolved easily in DI water at room temperature. This indicated the carboxymethylation process was successful since unmodified methyl cellulose does not dissolve easily in water at room temperature.

2.5. Experimental techniques

2.5.1. Potentiometric and conductometric titration

Simultaneous measurements of pH and conductivity were performed using the Metrohm 809 Titrando autotitrator. It is equipped with Tiamo software capable of dosing microlitres of any titrant. All measurements were conducted in a jacketed vessel at 25 °C with medium stirring. Initially, the pH of the microgel sample (0.1 wt%) was increased to 11 by adding NaOH. The sample was then titrated with 0.1 N HCl and the pH and conductivity were measured simultaneously until the pH of the sample approached 2. The pH and conductivity curves showed different transition points confirming the presence of $-OCH_2COOH$ and $-NH_2$ functional groups on the synthesized microgels.

2.5.2. Zeta potential measurements

Zeta potential measurements of the microgel samples at different pH values were measured using the Brookhaven ZetaPALS Analyzer, which uses the Phase Analysis Light Scattering principle to quantify the zeta potential and electrophoretic mobility. The concentration of the samples was maintained at ~0.1 wt% and the experiment was conducted at 25 °C.

2.5.3. Dynamic light scattering

Dynamic light scattering measurements were conducted at 25 °C using the BI-200SM goniometer for scattering detection at multiple angles. It is also equipped with BI9000AT digital correlator and BI-DNDC for static light scattering measurements as well. Laser with a wavelength of 636 nm was used. Microgel samples (0.1 wt%) at different pH values were used for measuring the hydrodynamic radii. In order to eliminate the effect of dust particles, a 0.45 μm filter was used to filter the samples prior to the measurements.

2.5.4. Surface tension measurements

Unmodified methyl cellulose (MC) and modified MC samples exhibited surface activity when the solutions were shaken or stirred. Hence, surface tension measurements were conducted for unmodified methyl cellulose and modified methyl cellulose samples. Since modified MC samples consist of carboxylic acid groups, it was expected that the surface activity of the modified samples depended on pH. The measurements were conducted in a DCAT11 (Dataphysics) tensiometer at 25 °C. It is equipped with a state-of-art software package and two liquid dispensing units (LDU) capable of dosing microlitres of titrant. Wilhelmy plate method was used to measure the dynamic surface tension values of the samples. The concentration of methyl cellulose and modified methyl cellulose samples were kept at 2 g/L and the polymers were titrated into 50 mL of DI water in 30 volumetric increments.

2.5.5. Differential scanning calorimetry

Microcal VP-DSC instrument was used to determine the thermoresponsive properties of unmodified and modified methyl cellulose samples. 0.5 wt% of the degassed samples were used in the sample cell along with DI water as the reference liquid. The experiments were conducted at constant pressure of ~27 psi. All upscan runs (from low to high temperature) were recorded.

2.5.6. FTIR

Bio-Rad (Excalibur series) FTIR spectrometer was used to analyze the modified and unmodified methyl cellulose samples. The wavelength range considered is 400–4000 cm^{-1}. KBr powder was mixed with the powder samples to make thin FTIR films by compressing them between steel platens.

2.5.7. Drug loading

To 60 mL of 0.1 wt% CS–CMC microgel solution, 163.66 mg PrHy was added to yield a concentration of 10 mM. The drug–microgel solution was stirred overnight at 25 °C and equilibrated for 24 h at room temperature. The drug–microgel solution was then passed through the stirred ultrafiltration cell (Millipore Corporation, Bedford, USA) with filters having a cut-off pore size of 25 nm (Millipore, VSWP, Ireland). The concentration of free PrHy in the filtrate was measured using a drug selective electrode (DSE). Electromotive force EMF measurements were recorded by the titration system with a built-in micro-voltometer. The electrode potential was recorded as a function of PrHy concentration (log [PrHy]) and calculated based on the calibration curves of EMF (mV) against concentration of PrHy in logarithmic scale from 10^{-4} to 10^{-1} M.

2.5.8. In vitro release studies

3 mL of filtered PrHy loaded microgels (0.84 wt%) was added to a double walled jacketed vessel containing 100 mL 10 mM NaCl solution at pH 7 and at a constant temperature of 25 °C with gentle stirring at 300 rpm. The in vitro drug release profile of CS–CMC microgels was determined using the DSE. A data acquisition software was used to acquire the EMF measurements at intervals of 20 s.

2.5.9. Transmission electron microscopy (TEM)

Transmission electron microscopic (TEM) images of CS–CMC microgel at different pHs were captured using a Philips CM10 TEM with 60 keV acceleration voltage. Approximately 10 μL of dilute aqueous suspensions of the samples were deposited on carbon-Formvar film on 200 mesh copper electron microscopic grids and the grids were allowed to dry. The grids were subsequently negatively stained with a 1 wt% phosphotungstic acid solution in ethanol.

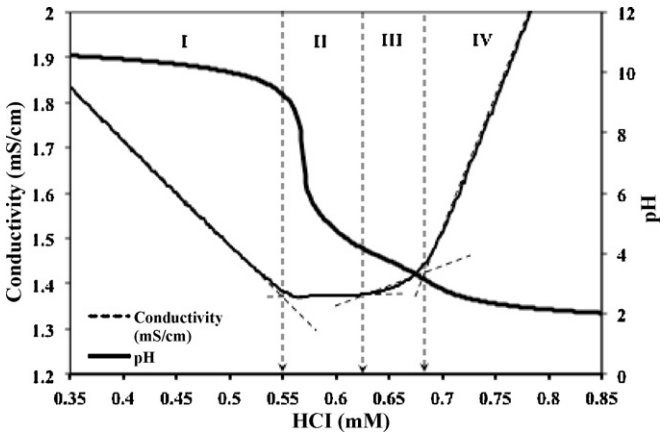

Fig. 1. pH and conductivity titration curve for 0.1 wt% CS–CMC microgels.

3. Results and discussion

3.1. Chitosan–carboxymethyl cellulose microgels (CS–CMC)

Fig. 1 shows the potentiometric and conductometric titration curve of 0.1 wt% CS–CMC microgel solution. At the start of the experiment, the sample was adjusted to pH 11 and then titrated with 0.1 M HCl. Different transition points on the pH and conductivity curves confirmed the presence of amino and carboxylic acid groups on the microgels. Transition points on the conductivity curve were determined by the change in slope (inflection points) and the intersection of vertical dashed lines with the pH curve is described as a transition point on the pH curve. For this system, the transition points on the pH curve were observed at pH of 9.4, 4.2 and 3.2. The titration curve exhibits four distinct regions: the first region (starting from left) corresponds to the neutralization of excess base. The second region (pH 9.4–4.2) corresponds to the protonation of $-OCH_2COO^-$ groups on the carboxymethyl cellulose (CMC) chains in the microgels. The third region (pH 4.2–3.2) corresponds to the protonation of $-NH_2$ groups on the chitosan (CS) chains in the microgels and finally the fourth region corresponds to excess acid present in the solution.

In terms of transition points on the pH curve, the first transition point at pH of 9.4 represents the start of protonation of $-OCH_2COO^-$ groups to $-OCH_2COOH$. This protonation ends at the second transition point, pH of 4.2. This point also corresponds to the start of protonation of $-NH_2$ groups to $-NH_3^+$. At the third transition point of pH 3.2, the protonation of $-NH_2$ groups is complete. By measuring the moles of HCl reacted for each functional group (second and third transition regions), the amount of $-OCH_2COOH$ and $-NH_2$ groups was determined as 1.5 and 1.1 meq/g of microgel.

Fig. 2A–D shows the hydrodynamic radii and zeta potentials at different pH values. As shown in Fig. 2A, for intermediate pH ranges between pH 4 and 9, a typical U-shaped profile was obtained for the hydrodynamic radius. At low pH, the $-NH_2$ groups on CS chains in the microgel are positively charged due to the protonation of amine groups. Due to the repulsion between $-NH_3^+$ groups on CS chains, the microgel swells and increases in size. Similarly, at high pH, the $-OCH_2COOH$ groups on CMC chains are negatively charged due to deprotonation of carboxylic acid groups. Therefore, the repulsion between $-OCH_2COO^-$ groups on CMC chains induces the swelling of the microgel. At neutral pH, the microgel exhibits an overall neutral charge and the microgel deswells and shrinks in size.

As shown in Fig. 2C, at extreme pH values (pH < 4 and pH > 10), the size of the microgels decreases somewhat, thus this trend cannot be attributed to charge shielding alone. This behaviour could be related to the acid and base catalyzed hydrolysis of amide linkages within the microgel. Once the amide crosslinks are hydrolyzed at extreme pH values, the CS and CMC chains are expelled from the microgels causing the microgel to decrease in size. Several papers have reported on the hydrolysis of amide bonds under acidic, basic and neutral conditions (Kahne & Still, 1988; Smith & Hansen, 1998; Zahn, 2004); it was observed that the rate of amide hydrolysis was higher at extreme pH values (i.e. pH < 4 and pH > 10) than at the neutral pH range, where the amide hydrolysis was slower.

The zeta potential values also corroborate with the above results. In the pH range of 4–9 (Fig. 2B), the surface charge on the particles decreases from +10 mV to −40 mV as the microgels possesses $-NH_3^+$ and $-OCH_2COO^-$ groups at low and high pH,

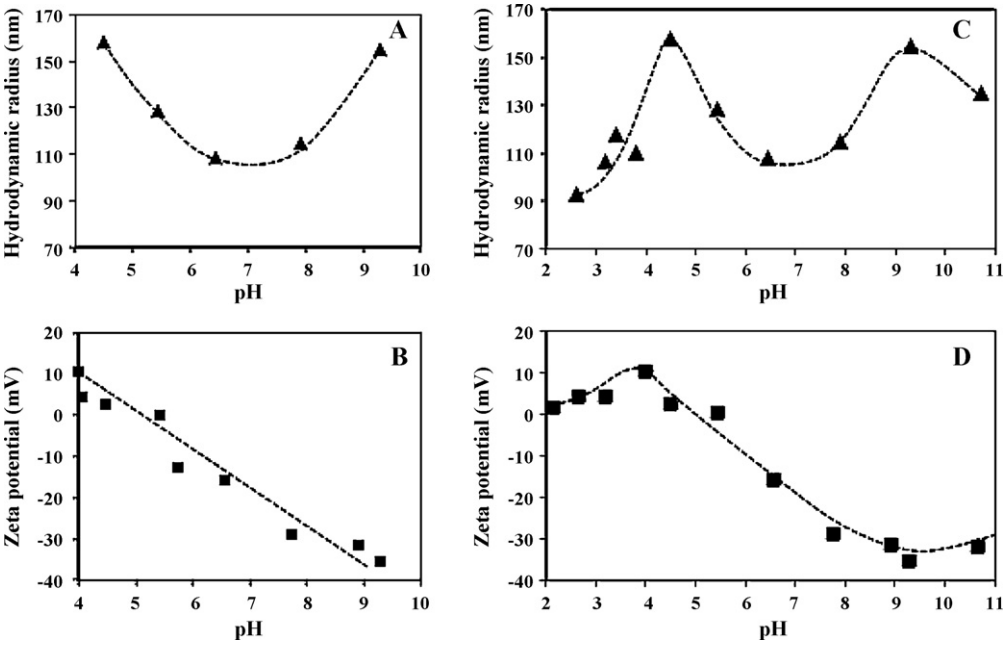

Fig. 2. Hydrodynamic radius (A) vs. intermediate pH range (4–9), zeta potential (B) vs. intermediate pH range (4–9), hydrodynamic radius (C) vs. entire pH range and zeta potential (D) vs. entire pH range for 0.1 wt% CS–CMC microgels.

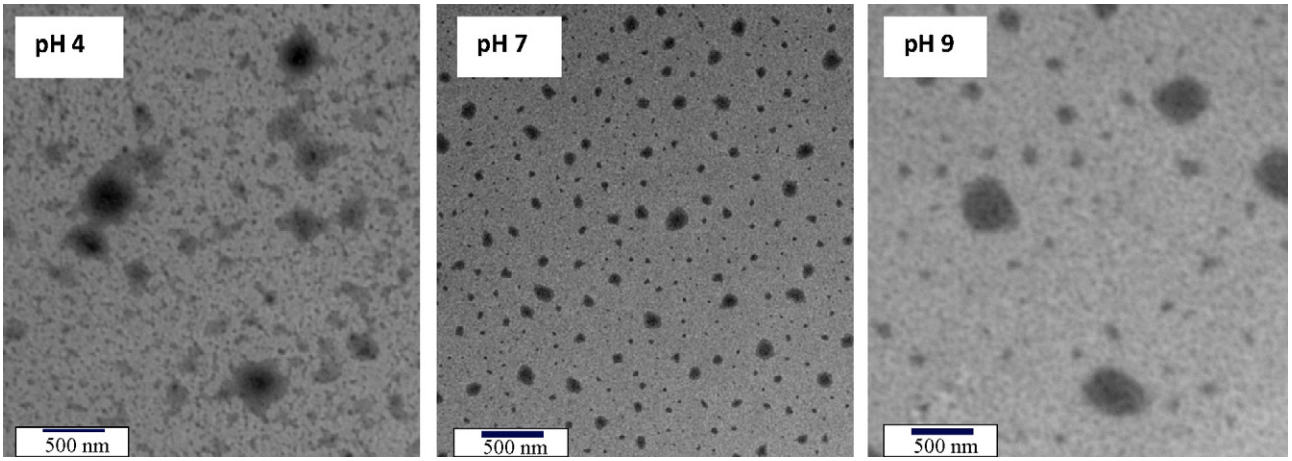

Fig. 3. Transmission electron microscopic (TEM) micrographs of CS–CMC microgels at three different pH values, i.e. pH 4, pH 7, and pH 9.

respectively. However, at pH < 4 and pH > 10 (Fig. 2D), the charge on the microgel particle decreases, suggesting the expulsion of CS and CMC chains due to acid and base catalyzed amide bond hydrolysis.

Another important observation that could be derived from the zeta potential values is shown in Fig. 2B. While the maximum negative charge on the microgels is −40 mV, the maximum positive charge on the microgels is only +10 mV. This might seem contradictory since the amounts of $-NH_2$ groups (1.1 meq/g) are comparable to the amount of $-OCH_2COOH$ groups (1.5 meq/g). Zeta potential analyzer measures only the surface charge on a particle and some of the surface $-NH_2$ groups are involved in PEGMA grafting; thereby lowering the positive zeta potential values.

Fig. 3 shows TEM micrographs of CS–CMC microgels at different pH values and the size of microgel is consistent with the DLS results. Furthermore, the particle size at pH 7 is smaller compared to particle sizes at pH 4 and 9, confirming the deswelling at neutral pH and the swelling of the microgel in acidic and basic pH, respectively.

Procaine hydrochloride (PrHy) a widely known local anesthetic was chosen as a model drug for in vitro drug release studies. The encapsulation efficiency of microgels and drug loading were determined indirectly by measuring the free drug not captured in the medium. From the expression below, the encapsulation efficiency and drug loading were determined:

$$\text{Encapsulation efficiency}\,(\%) = \frac{\text{weight of drug loaded}}{\text{weight of drug in microgel}} \times 100$$

$$\text{Drug loading} = \frac{\text{weight of drug loaded}}{\text{weight of microgels}}$$

For CS–CMC microgels the encapsulation efficiency and drug loading were 39.1% and 0.016 g/g, respectively. Similar entrapment efficiency (47.6–63%) was reported for crosslinked chitosan nanoparticles for Timolol maleate drug (Agnihotri & Aminabhavi, 2007). Due to the rigid backbones of CS and CMC polymers, the microgel particles form a loose crosslinked network leading to a lower encapsulation efficiency of PrHy.

Fig. 4 shows the in vitro release studies of the PrHy loaded CS–CMC microgels at pH 7. It shows a relatively fast release of PrHy in the first half an hour (burst release) followed by a slower release of the remaining drug in about 4 h. The initial burst release could be due to drug on the surface of microgels, and also the lower chain density near the surface of the microgel, while the slower release could be due to higher density of crosslinked chains at the microgel core thereby inhibiting drug diffusion. The ratio of M_t/M_∞ is the molar ratio of drugs released at time t and the drugs that partition to the microgel particles. The drug release profile obtained is similar to previously reported study on the kinetics of procaine hydrochloride release from pH-responsive microgels (Tan, Zeng, Chang, & Tam, 2008). A similar system comprising of interpenetrating networks of chitosan and hydroxyethyl cellulose was explored to study the release of isoniazid drug (Angadi, Manjeshwar, & Aminabhavi, 2010). In this system, a maximum drug release ~75% was observed for 16 h with a maximum encapsulation efficiency of 66%. In comparison, CS–CMC system showed a ~100% drug release in 4 h with an encapsulation efficiency of 39.1%. This observed faster drug release for CS–CMC microgels compared to chitosan and hydroxyethyl cellulose IPN microgels is probably due to the loosely crosslinked CS–CMC microgels allowing faster diffusion of drugs through the drug delivery matrices.

3.2. Modified methyl cellulose (Mod-MC)

This section discusses the modified MC system that was synthesized for the subsequent preparation of the CS–ModMC microgel system. Fig. 5A shows the FTIR spectra of (i) methyl cellulose and (ii) modified methyl cellulose. The spectra for modified MC shows the characteristic C=O frequency at 1750 cm^{-1} confirming the presence of carboxymethyl groups on MC chains.

Fig. 5B shows the zeta potential results for modified MC samples at different pH values. As expected, the zeta potential values become more negative at higher pH values due to the deprotonation of carboxymethyl groups on the modified MC chains. Fig. 5C shows the potentiometric and conductometric titration curve for 0.1 wt% modified MC sample. Intersection of vertical dashed lines

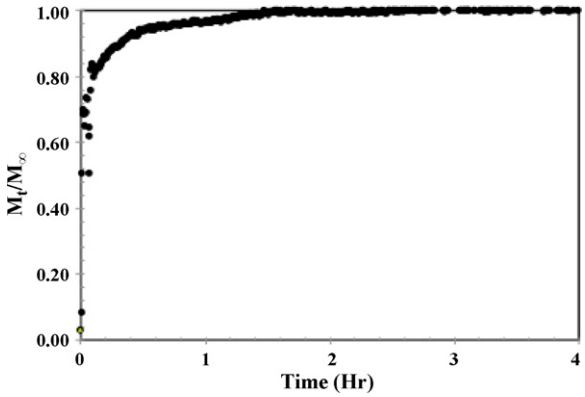

Fig. 4. In vitro release profile for procaine hydrochloride from CS–CMC microgels at pH 7.

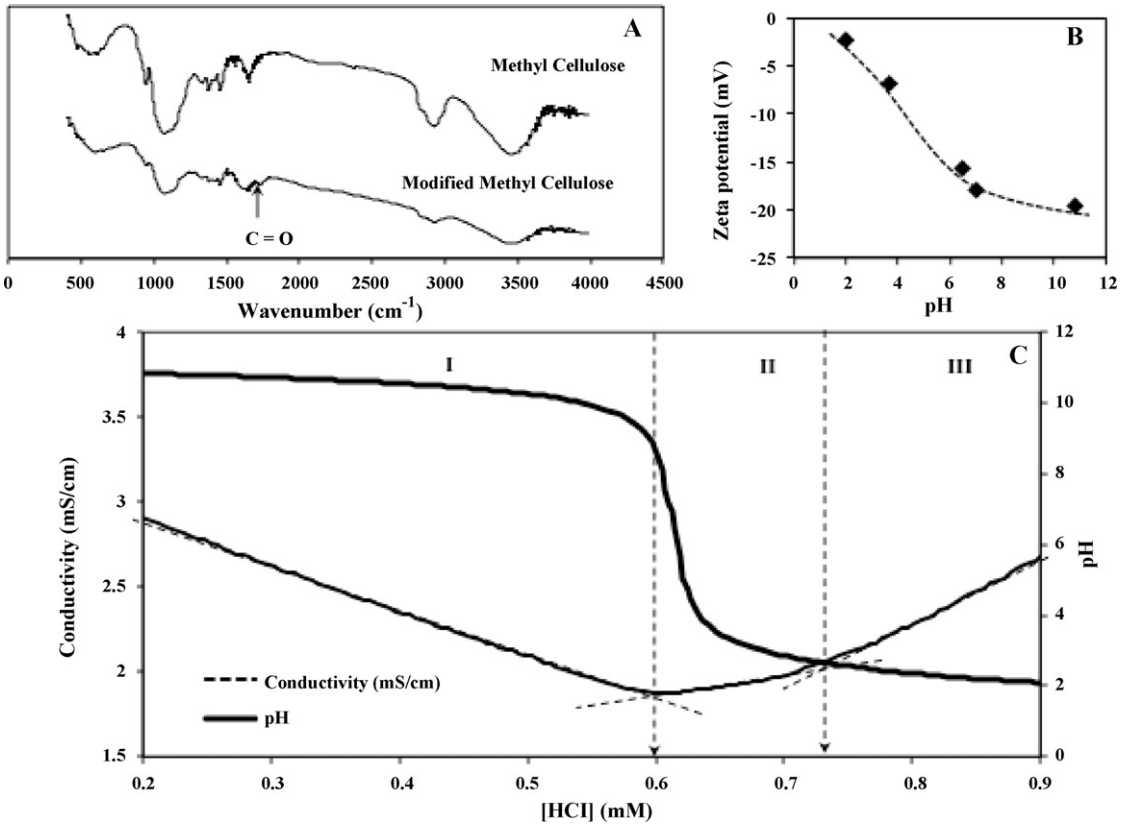

Fig. 5. (A) FTIR of methyl cellulose and modified methyl cellulose, (B) zeta potential vs. pH for modified MC sample and (C) pH and conductivity vs. [HCl] for 0.1 wt% modified MC sample.

with the pH curve represents the transition point on the pH curve. The first region (starting from left) corresponds to excess OH^- ions, while the second region represents the protonation of $-OCH_2COO^-$ groups to $-OCH_2COOH$ (pH 9–3). The third region corresponds to excess HCl. By measuring the moles of HCl in the second transition region, the no. of $-OCH_2COOH$ groups was determined to be 2.6 meq/g of sample.

We observed that unmodified and modified MC solutions exhibited surface activity when they were subjected to stirring/shaking. Fig. 6 shows the surface tension results for unmodified and modified MC samples. The inset shows an expanded region of the data at higher concentration of modified MC. The surface tension of unmodified MC sample decreases as the concentration of the polymer is increased, suggesting that the unmodified MC samples are surface active (Fig. 6). We hypothesize that unmodified MC chains partition to the air–water interface, where the hydrophobic methoxide groups extends towards the non-aqueous air phase. Fig. 7A shows a schematic on the orientation of hydrophobic methoxide groups at the air–water interface. When the polymer concentration is increased, a higher proportion of hydrophobic methoxide groups induced the aggregation of MC chains at the interface causing the surface tension values to decrease further. Unmodified MC sample contains significantly higher fractions of hydrophobic methoxide groups ($-OCH_3$), such that they preferentially partition to the air–water interface resulting in the apparent surface-active character of unmodified MC. Since unmodified MC shows surface activity similar to surfactants, we expect to observe a critical micelle concentration (cmc) as defined by a transition in the surface tension profile. However, no cmc transition was observed for unmodified MC, suggesting that the polymer does not self-associate into micellar aggregates.

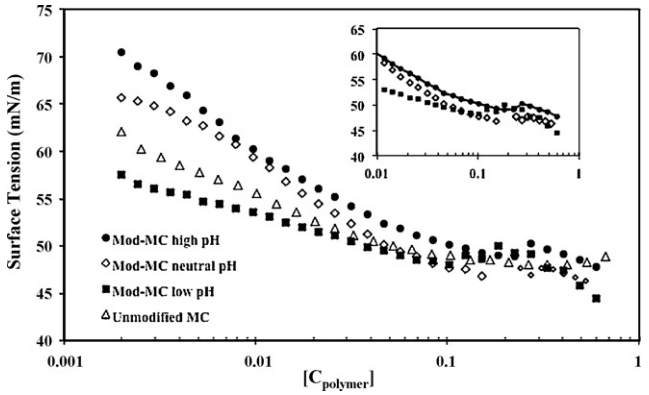

Fig. 6. Surface tension curves for unmodified MC and modified MC at low, neutral pH and high pH.

While unmodified MC chains are unresponsive to changes in pH, the presence of carboxymethyl groups on modified MC chains makes them pH –responsive, and varying the pH affects the degree of deprotonation of $-OCH_2COOH$ groups on modified MC chains. This effect is clearly seen in Fig. 6, where the surface tension curves for modified MC samples at different pH values show similar trends but their absolute values are different. For all modified MC samples at different pH values, the surface tension values decrease with increasing polymer concentrations indicating that the modified MC samples show surface activity at low, neutral and high pH.

For modified MC sample at low pH, the surface tension values are lower than those of unmodified MC sample suggesting that the modified sample at low pH is more surface active than unmodified MC. At low pH, the carboxymethyl groups in modified MC are protonated to $-OCH_2COOH$. Both hydrophobic methoxide

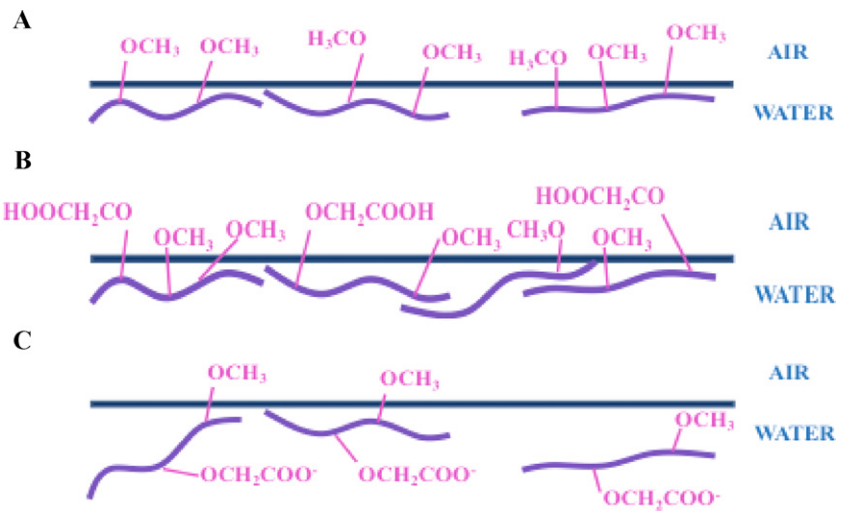

Fig. 7. (A) Unmodified MC chains at air–water interface, (B) modified MC chains (low pH) at air–water interface and (C) modified MC chains (neutral pH) at air–water interface.

($-OCH_3$) and the $-OCH_2COOH$ groups preferentially partition to the air–water interface (see Fig. 7B) thereby decreasing the surface tension of the solution. The partitioning of –COOH groups of linear polyelectrolytes to the air–liquid interface was also proposed by Okubo and Kobayashi (Okubo & Kobayashi, 1998). Due to partitioning of $-OCH_2COOH$ and $-OCH_3$ groups to the air–water interface, at low pH, modified MC sample exhibits more surface activity than unmodified MC sample.

At neutral pH, modified MC sample possesses higher surface tension values than unmodified MC sample suggesting that there is less surface activity for modified MC sample. At neutral pH, a fraction of the carboxymethyl groups are deprotonated to $-OCH_2COO^-$ groups and these charged groups remain in the aqueous phase (see Fig. 7C). Thus, hydrophobic methoxide groups on modified MC chains are less prone to partition to the air–water interface resulting in a lower surface activity.

Similarly at high pH, most carboxymethyl groups on modified MC chains are deprotonated to $-OCH_2COO^-$ groups, which are hydrophilic. Hence, the surface activity of modified MC is further decreased at high pH in comparison to unmodified MC sample. Similar to the unmodified MC sample, the modified MC samples did not show any cmc transition point for low, neutral and high pH.

3.3. Chitosan–modified methyl cellulose microgels (CS–ModMC)

Fig. 8 shows the potentiometric and conductometric titration curves for CS–ModMC microgel system. The intersection of vertical dashed lines with the pH curve represents the transition point on the pH curve. The titration curve exhibits three transitions points at pH of 9.5, 5.5 and 3.8. Region I represents the presence of excess base in the sample. The second region (pH 9.5–5.5) corresponds to the start of the protonation of $-OCH_2COO^-$ to $-CH_2COOH$ groups on the modified MC chains in the microgel. The third region (pH 5.5–3.8) corresponds to the end of protonation of $-OCH_2COO^-$ and the start of protonation of $-NH_2$ to $-NH_3^+$. The fourth region corresponds to the end of protonation of $-NH_2$ groups on the CS chains and the presence of excess HCl in the sample. By measuring the moles of HCl reacted for each functional group (second and third transition regions), the amount of $-OCH_2COOH$ and $-NH_2$ groups were determined as 0.8 and 0.6 meq/g of the microgel, respectively.

Fig. 9 shows the hydrodynamic radius and the zeta potentials of CS–ModMC microgels at different pH values. In the pH range of 4–9, the microgels exhibit swelling at low and high pH and deswelling at neutral pH. However, for pH < 4 and pH > 10, the size of microgel

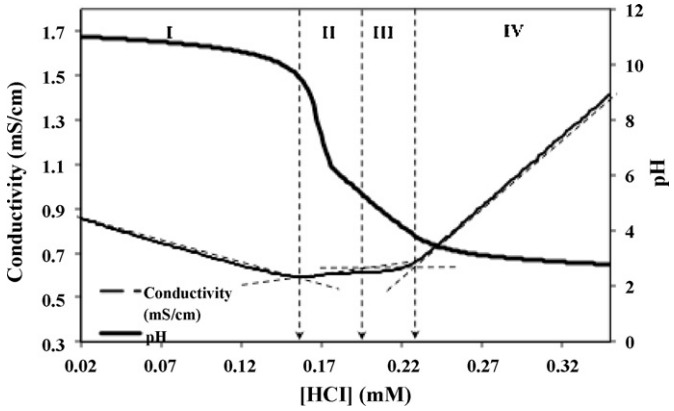

Fig. 8. pH and conductivity titration curve for 0.1 wt% CS–ModMC microgels.

decreases again probably due to acid and base catalyzed hydrolysis of amide bonds. The zeta potential values also corroborate with the above results since the surface charge on the microgels is lowered at extreme pH values. The isoelectric point (IEP) from hydrodynamic radius measurements is ~7 while the IEP from zeta potential measurements is ~6.4.

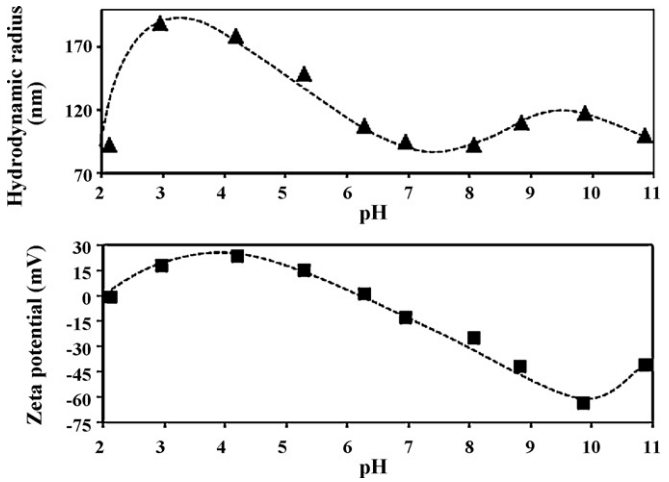

Fig. 9. Hydrodynamic radius and zeta potential vs. pH for 0.1 wt% CS–ModMC microgels.

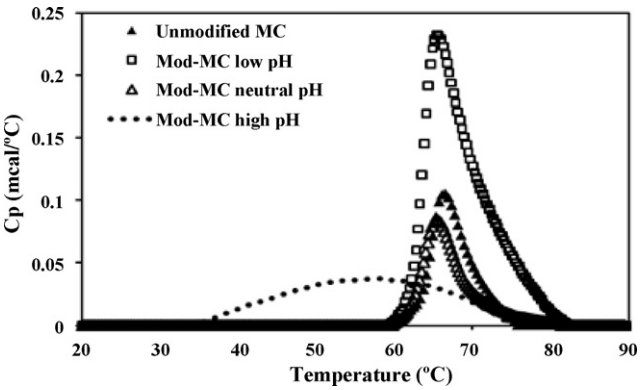

Fig. 10. Upscan DSC curves for unmodified and modified MC samples.

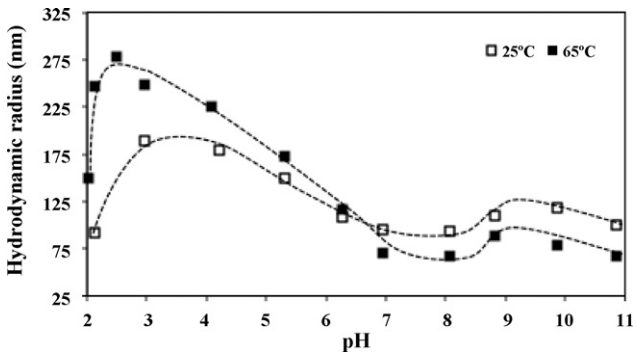

Fig. 11. Hydrodynamic radii vs. pH at 25 and 65 °C for CS–ModMC microgels.

However, the zeta potentials shown in Fig. 9 shows that the particles are significantly more negative at high pH values and less positive at lower pH values, suggesting the presence of more $-OCH_2COOH$ groups compared to $-NH_2$ groups in the microgel. This may seem contradictory to the amount of $-OCH_2COOH$ and $-NH_2$ groups determined from Fig. 8, which have comparable values at 0.8 and 0.6 meq/g of the microgel, respectively. This discrepancy may be explained from the fact that most surface $-NH_2$ groups are utilized in PEGMA grafting reaction resulting in lower zeta potential values at low pH. Also, Fig. 9 reveals that the amount of swelling at lower pH values is greater in comparison to that observed at high pH values. This may be explained by the presence of the chitosan chains (CS) in the core of the microgel and the presence of modified methyl cellulose (ModMC) chains at the surface of the microgel; hence, the presence of $-NH_2$ groups in the microgel core induces greater swelling at lower pH values while the $-OCH_2COOH$ groups on the microgel surfaces results in a more negatively charged particle at higher pH values.

3.3.1. *Thermoresponsive behaviour of CS–ModMC microgels*

When aqueous methyl cellulose solutions were heated above a critical temperature called the lower critical solution temperature (LCST), the hydrophobic methoxide groups ($-OCH_3$) in methyl cellulose self-associate. Thus, unmodified methyl cellulose solutions exhibit thermoresponsive behaviour at LCST (Chevillard & Axelos, 1997). Since CS–ModMC microgels contain methoxide groups ($-OCH_3$), the microgels are expected to exhibit thermo-responsive characteristic as well. In order to study the thermoresponsive behaviour of CS–ModMC microgels, the LCST of modified MC samples was determined by microcalorimetry (see Fig. 10) and a characteristic LCST peak was observed at around 65 °C. The hydrodynamic radii (R_h) vs. pH measurements were repeated for CS–ModMC microgels at the LCST of 65 °C. By comparing the R_h vs. pH behaviours at 25 and 65 °C (see Fig. 11), the thermoresponsive character of CS–ModMC microgels was confirmed.

Fig. 10 shows the upscan results for unmodified and modified MC samples determined using a micro-calorimeter. Modified MC samples were studied at different pH values to analyze the effect of carboxymethyl groups on the hydrophobic association between modified MC chains. For unmodified MC sample, the LCST peak occurred at around 65 °C. For the modified MC sample at low pH, a similar LCST peak at 65 °C was observed. However, the peak for modified MC sample at low pH is larger compared to the peak of unmodified MC sample. At low pH values, protonation of carboxymethyl groups to $-OCH_2COOH$ groups facilitates hydrogen bonding between $-OCH_2COOH$ and $-OCH_3$ groups while weakening the hydrophobic interactions between $-OCH_3$ groups. Therefore, more energy is required to induce hydrophobic interactions between the modified MC chains at low pH; hence the LCST peak for the modified MC sample is larger compared to the unmodified MC sample. For modified MC sample at neutral pH, LCST peak was again observed at around 65 °C. At neutral pH, deprotonation of $-OCH_2COOH$ groups to $-OCH_2COO^-$ reduces the hydrogen bonding between $-OCH_2COOH$ and $-OCH_3$ groups and facilitates the hydrophobic interactions between $-OCH_3$ groups. Hence, less energy is required to induce hydrophobic interactions between the modified MC chains at neutral pH, thereby reducing the LCST peak. Similarly, at high pH, most of the carboxymethyl groups on modified MC chains are deprotonated to $-OCH_2COO^-$ groups. So, the hydrogen bonding between $-OCH_2COOH$ and $-OCH_3$ groups is further weakened and the hydrophobic interactions between $-OCH_3$ groups are further strengthened. At high pH, we see a broad LCST peak at ~55 °C, which is probably due to the enhanced hydrophobic interactions and gelling phenomena in the modified MC sample.

Fig. 11 shows a comparison of the hydrodynamic radii vs. pH at 25 and 65 °C. The CS–ModMC microgels are polyampholytic and possess pH-responsive behaviour at both temperatures. While the response profiles are similar at both temperatures, we observe a difference in the values of hydrodynamic radii (R_h) at the two temperatures. At low pH values (pH < 6.5), the R_h values at 65 °C are higher compared to those at 25 °C. At higher pH values (pH > 6.5), the R_h values at 65 °C are lower compared to those at 25 °C. Similar to micro-DSC results for modified MC samples, this behaviour may be explained by the degree of deprotonation of modified MC chains in the microgel. At low pH, the hydrogen bonding between $-OCH_2COOH$ and $-OCH_3$ groups prevents the hydrophobic interactions between $-OCH_3$ groups. So, a large number of water molecules are partitioned to the porous microgel and surrounded the $-OCH_3$ groups. Thus, the microgel particles at 65 °C swell more and show larger hydrodynamic radii in comparison to the microgels at 25 °C. Conversely at high pH, due to deprotonation of $-OCH_2COOH$ to $-OCH_2COO^-$ groups, the hydrogen bonding between $-OCH_2COOH$ and $-OCH_3$ groups is weakened while the hydrophobic interaction between $-OCH_3$ groups is enhanced. Water molecules are no longer surrounding the $-OCH_3$ groups in the CS–ModMC microgel and are excluded from the microgel. Therefore, microgel particles at 65 °C have smaller hydrodynamic radii compared to the microgels at 25 °C.

4. Conclusions

Two different biocompatible microgel systems were synthesized using chitosan, carboxy methyl cellulose and modified methyl cellulose. Polyampholytic microgels from chitosan-CMC and chitosan–modified methyl cellulose were prepared using an inverse microemulsion technique. pH responsive behaviour was observed in chitosan–carboxymethyl cellulose microgel system. Furthermore, methyl cellulose was modified using carboxymethylation and incorporated in the microgel along with chitosan.

pH and temperature responsive behaviours were observed in chitosan–modified methyl cellulose microgel system. Expulsion of polymeric chains from the microgels was observed at extreme pH values probably due to the hydrolysis of amide crosslinks. In vitro drug release studies indicate that these microgels systems could be used as biocompatible and biodegradable fast response drug carriers.

Acknowledgements

The financial support provided by the University of Waterloo has enabled Neha Dhar to pursue her graduate study. KC Tam would like to acknowledge the support from CFI and NSERC. We wish to thank Dr. Penlidis for the use of the zeta potential analyser.

References

Agnihotri, S. A., & Aminabhavi, T. M. (2007). Chitosan nanoparticles for prolonged delivery of timolol maleate. *Drug Development and Industrial Pharmacy*, *33*, 1254–1262.

Agnihotri, S. A., Mallikarjuna, N. N., & Aminabhavi, T. M. (2004). Recent advances on chitosan-based micro-and nanoparticles in drug delivery. *Journal of Controlled Release*, *100*, 5–28.

Angadi, S. C., Manjeshwar, L. S., & Aminabhavi, T. M. (2010). Interpenetrating polymer network blend microspheres of chitosan and hydroxyethyl cellulose for controlled release of isoniazid. *International Journal of Biological Macromolecules*, *47*, 171–179.

Chen, H., & Fan, M. (2008). Novel thermally sensitive pH-dependent chitosan/carboxymethyl cellulose hydrogels. *Journal of Bioactive and Compatible Polymers*, *23*, 38–48.

Chevillard, C., & Axelos, M. A. V. (1997). Phase separation of aqueous solution of methylcellulose. *Colloid and Polymer Science*, *275*, 537–545.

Christodoulakis, K. E., & Vamvakaki, M. (2010). Amphoteric core-shell microgels: Contraphilic two-compartment colloidal particles. *Langmuir*, *26*, 639–647.

Das, M., & Kumacheva, E. (2006). From polyelectrolyte to polyampholyte microgels: Comparison of swelling properties. *Colloid Polymer Science*, *284*, 1073–1084.

Heinze, T., & Koschella, A. (2005). Carboxymethyl ethers of cellulose and starch—A review. *Macromolecular Symposia*, *223*, 13–39.

Heinze, T., & Pfeiffer, K. (1999). Studies on the synthesis and characterization of carboxymethylcellulose. *Angewandte Makromolekulare Chemie*, *266*, 37–45.

Ho, B. S., Tan, B. H., Tan, J. P. K., & Tam, K. C. (2008). Inverse microemulsion polymerization of sterically stabilized polyampholyte microgels. *Langmuir*, *24*, 7698–7703.

Kahne, D., & Still, W. C. (1988). Hydrolysis of a peptide-bond in neutral water. *Journal of the American Chemical Society*, *110*, 7529–7534.

Kamel, S., Ali, N., Jahangir, K., Shah, S. M., & El-Gendy, A. A. (2008). Pharmaceutical significance of cellulose: A review. *Express Polymer Letters*, *2*, 758–778.

Lehnert, S., Tarabishi, H., & Leuenberger, H. (1994). Investigation of thermal phase inversion in emulsions. *Colloids and Surfaces A-Physicochemical and Engineering Aspects*, *91*, 227–235.

Mansour, O. Y, Nagaty, A., & Elzawawy, W. K. (1994). Variables affecting the methylation reactions of cellulose. *Journal of Applied Polymer Science*, *54*, 519–524.

Nakajima, N., & Ikada, Y. (1995). Mechanism of amide formation by carbodiimide for bioconjugation in aqueous-media. *Bioconjugate Chemistry*, *6*, 123–130.

Neyret, S., & Vincent, B. (1997). The properties of polyampholyte microgel particles prepared by microemulsion polymerization. *Polymer*, *38*, 6129–6134.

Oh, J. K., Drumright, R., Siegwart, D. J., & Matyjaszewski, K. (2008). The development of microgels/nanogels for drug delivery applications. *Progress in Polymer Science*, *33*, 448–477.

Okubo, T., & Kobayashi, K. (1998). Surface tension of biological polyelectrolyte solutions. *Journal of Colloid and Interface Science*, *205*, 433–442.

Rinaudo, M. (2008). Main properties and current applications of some polysaccharides as biomaterials. *Polymer International*, *57*, 397–430.

Samir, M. A. S. A., Alloin, F., & Dufresne, A. (2005). Review of recent research into cellulosic whiskers, their properties and their application in nanocomposite field. *Biomacromolecules*, *6*, 612–626.

Schachschal, S., Balaceanu, A., Melian, C., Demco, D. E., Eckert, T., Richtering, W., et al. (2010). Polyampholyte microgels with anionic core and cationic shell. *Macromolecules*, *43*, 4331–4339.

Smith, R. M., & Hansen, D. E. (1998). The pH-rate profile for the hydrolysis of a peptide bond. *Journal of the American Chemical Society*, *120*, 8910–8913.

Tan, B. H., & Tam, K. C. (2008). Review on the dynamics and micro-structure of pH-responsive nano-colloidal systems. *Advances in Colloid Interface Science*, *136*, 25–44.

Tan, B. H., Ravi, P., Tan, L. N., & Tam, K. C. (2007). Synthesis and aqueous solution properties of sterically stabilized pH-responsive polyampholyte microgels. *Journal of Colloid and Interface Science*, *309*, 453–463.

Tan, J. P. K., Zeng, A. Q. F., Chang, C. C., & Tam, K. C. (2008). Release kinetics of procaine hydrochloride (PrHy) from pH-responsive nanogels: Theory and experiments. *International Journal of Pharmaceutics*, *357*, 305–313.

Wang, X., Zhang, L., Wang, L., Sun, J., & Shen, J. (2010). Layer-by-layer assembled polyampholyte microgel films for simultaneous release of anionic and cationic molecules. *Langmuir*, *26*, 8187–8194.

Xu, K., Tan, Y., Chen, Q., An, H., Li, W., Dong, L., et al. (2010). A novel multi-responsive polyampholyte composite hydrogel with excellent mechanical strength and rapid shrinking rate. *Journal of Colloid and Interface Science*, *345*, 360–368.

Yoon, D. S., Cho, Y. K., Oh, K. W., Kim, S., Kim, Y. A., Han, J. I., et al. (2006). A microfluidic gel valve device using reversible sol-gel transition of methyl cellulose for biomedical application. *Microsystem Technologies-Micro-and Nanosystems-Information Storage and Processing Systems*, *12*, 238–246.

Zahn, D. (2004). On the role of water in amide hydrolysis. *European Journal of Organic Chemistry*, 4020–4023.